



## Seismic Assessment of First and Second Secant Stiffness for the Masonry Infilled RC Frame

Abhijeet A. Galatage <sup>1\*</sup>, Satish B. Patil <sup>1</sup>

<sup>1</sup> Department of Civil Engineering, School of Engineering and Sciences, MIT Art, Design and Technology University, Pune, Maharashtra 412201, India.

Received 25 October 2024; Revised 19 January 2025; Accepted 24 January 2025; Published 01 February 2025

### Abstract

The seismic resilience of composite concrete frame structures composed with masonry infill walls, is a critical research area due to its impact on structural performance during earthquakes. Most studies on reinforced concrete (RC) frames focus on key seismic response parameters like lateral strength and overall hysteretic behavior under cyclic loading, often analyzing the first and second secant stiffness throughout the seismic loading process. The present study examines the first and second secant stiffness as the structural performance during earthquake. A series of experimental tests are performed on half scaled RC frames filled with autoclaved aerated concrete (AAC) block masonry with external dimensions of 1.5 m x 1.5 m. These frames are subjected to displacements ranging from 2 mm to 6 mm and frequencies between 1 Hz and 7 Hz for simulating earthquake loading conditions. The experimental program aimed to evaluate the resistance of structure to earthquake loading by using dual mode of testing viz. displacement and frequency-controlled loading protocol. During test the RC frame responded elasto-plastically due to minor cracking at block joints and localized yielding at the interface between the frame and the infill at lower frequencies and displacements. Conversely the degradation of both first and second secant stiffness values became more pronounced at higher frequencies. The first secant stiffness decreased by 73.4%, while the second secant stiffness showed increase of 24.6% at a displacement of 4 mm and a frequency of 4 Hz with respect to the previous loading cycle which indicated the complex stress redistribution and temporary stabilization.

*Keywords:* Secant Stiffness; Seismic Loading; Infilled Frame; Frequency; Displacement; Energy Dissipation.

### 1. Introduction

The response of the framed concrete structures to the earthquake load is a matter of global importance since it is having huge impact on society as well as economy of the world. These frames can resist lateral loads during an earthquake and prevent structural collapse due to their in-plane strength and stiffness. However, cyclic loading, which is typically used to simulate the dynamic effects of seismic forces, often disrupts their structural performance. The variations in strength are often influenced by factors such as frequency, lateral displacement, and in-plane strength [1]. Understanding these discrepancies in structural performance is critical for seismic design and assessment, enabling engineers to predict structural responses under real earthquake scenarios and implement effective design strategies to enhance the flexibility and resilience of RC structures [1, 2].

Research highlights the significance of the initial rigidity of masonry-infilled frames and its gradual deterioration in comprehending the load-carrying capacity and structural stability of these systems during seismic events. Raj & Ravula [2] examined the mechanical behavior of autoclaved aerated concrete (AAC) block masonry, focusing on the influence

\* Corresponding author: [abhijeet.galatage@mituniversity.edu.in](mailto:abhijeet.galatage@mituniversity.edu.in)

<http://dx.doi.org/10.28991/CEJ-2025-011-02-05>



© 2025 by the authors. Licensee C.E.J, Tehran, Iran. This article is an open access article distributed under the terms and conditions of the Creative Commons Attribution (CC-BY) license (<http://creativecommons.org/licenses/by/4.0/>).

of masonry configuration and bonding material strength on stiffness characteristics. Their findings revealed that under high-frequency cyclic loading, stiffness degradation serves as an early indicator of potential structural failure. Similarly, Xi & Liu [1] investigated the seismic performance of RC frames with masonry infills, showcasing notable improvements in lateral load capacity and energy dissipation attributed to the inclusion of infills [1, 2]. Furthermore, studies by Zade et al. [3] and Furtado et al. [4] offer critical insights into stiffness degradation under cyclic loads, particularly emphasizing the impact of displacement-controlled loading protocols on stiffness reduction and their implications for seismic performance.

The study by Đorđević & Marinković [5] uses Artificial Neural Network (ANN) algorithms to predict the fundamental period of vibration for masonry-infilled RC frames. By analyzing 4,026 samples of bare and infilled frames, the research compares first and second-order ANN models, highlighting superior accuracy compared to traditional seismic design codes. This research reveals the underutilization of AI in predicting parameters such as secant stiffness degradation, indicating a gap in AI-driven seismic assessment for infilled frames. Despite the advancements in understanding the seismic behavior of masonry-infilled RC frames, the application of AI tools for predicting their response remains limited. Existing studies rely on traditional analytical and experimental methods. Integrating AI-based models like CNNs and LSTMs could enhance prediction accuracy, providing better alignment with modern seismic design frameworks. Addressing this gap could lead to more efficient and resilient structural designs under varying seismic conditions.

Structure of this research paper: This research paper is structured as follows: the Introduction outlines the study's objectives and scope, followed by a Literature Review that identifies existing research gaps and sets the foundation for the study. The Displacement-Based Analysis evaluates secant stiffness for displacements ranging from 2 mm to 6 mm, while the Frequency-Based Analysis examines stiffness variations from 1 Hz to 7 Hz, providing an in-depth assessment of the Hysteresis Behavior of Load vs. Displacement. The Methodology section details the Specimen Preparation, Testing Framework, and Loading Protocol. The paper concludes with a Summary of Findings, Conclusions, Declarations, and References.

## 2. Literature Review

Displacement-Based Design (DBD) approaches have emerged as a pivotal focus in seismic engineering, emphasizing the control of structural deformations during earthquake events. Sullivan et al. [6] observed that secant stiffness-based methods, such as CASPEC and DDBD, necessitate higher design strengths to effectively manage displacement ductility demands. This requirement often leads to larger base shear forces compared to initial stiffness-based methods like INSPEC and YPS. Research by Gaikwad et al. [7] demonstrated that RC frames subjected to high-frequency motions exhibited a 20% increase in lateral stiffness compared to those exposed to low-frequency motions, emphasizing the significant influence of loading rates on structural response. Additionally, their study revealed that taller structures (e.g., 18-story buildings) dissipated 15% more energy than shorter structures (e.g., 5-story buildings) due to enhanced stiffness and ductility. These findings are particularly relevant for evaluating the secant stiffness of masonry-infilled RC frames, which are highly susceptible to varying seismic conditions.

The performance of concrete frames with masonry infills on sloping ground, investigated by Sivanantham et al. [8], highlighted a 50% increase in in-plane strength and a 2.45-fold enhancement in energy dissipation under the short column effect and dynamic loading compared to bare frames. Furthermore, recent advancements indicate a growing interest in leveraging Artificial Intelligence (AI) to predict the seismic response of infilled frames, offering promising solutions for optimizing structural performance under dynamic conditions. Thisovithan et al. [9] developed an AI-based neural network algorithm to predict the fundamental period of masonry-infilled RC frames, showing improved accuracy over conventional methods. Similarly, Cattari et al. [10] validated a strut modeling approach for seismic response prediction but emphasized the need for simpler and more robust models. These studies highlight the underutilization of AI tools in accurately predicting the seismic behavior of masonry-infilled RC frames, presenting a significant research gap.

The lateral stiffness of fabric-reinforced cementitious matrix (FRCM) composites on RC frames with masonry infills was found to be increased by 30% and energy dissipation improved by 20-25% due to inclusion of FRCM layers by Wang et al. [11]. Blasi et al. [12] found that the ductility of the RC frame was reduced by 25% and lateral stiffness increased by 15% after increasing overstrength factor by 30% leading to brittle failure modes. This finding underlines the importance of considering infill properties during the design process. The research by Cai & Su [13] demonstrated that infills can improve lateral stiffness by up to 60% though proper selection of joining materials in determining ductility and overall performance of the structure. The use of buckling-restrained braces (BRBs) by Chen & Bai [14] in RC frames significantly enhanced the seismic resilience through improving lateral stiffness and energy dissipation by 40% and 30% respectively. On the contrary Furtado et al. [4] demonstrated that the openings in infill wall reduces initial stiffness by 20% indicating more structural vulnerability. The study by Kurmi et al. [15] explores the effect of realistic openings in masonry infills on the seismic performance of gravity-load designed RC buildings. It highlights that

openings significantly influence the stiffness and energy dissipation capacity of infilled frames, affecting their overall seismic response. The findings emphasize the need for accurate assessment of stiffness degradation in infilled frames with openings, which is relevant for evaluating first and second secant stiffness under seismic loading conditions. Liu et al. [16] investigate the seismic performance of corroded RC frames with masonry infills. The research demonstrates how corrosion affects the structural integrity and lateral stiffness of infilled frames, leading to premature failure. This study underscores the importance of incorporating deterioration effects into seismic analysis models to predict the realistic behavior of infilled RC frames accurately.

The dynamic response of buildings composed of light weight concrete block investigated by Rai & Joshi [17] investigated found 30% increase in resistance to lateral load carrying capacity compared to frames without masonry infill. The study by Zade et al. [3] shown that the infilled frames exhibited a 50% more strength in-plane direction and improved energy absorption compared to conventional clay brick infills. This study draw attention towards the use of AAC blocks for improving the dynamic response of reinforced concrete frame structures when considering displacement-based design (DBD) methods as described in FEMA 306 and FEMA 440 guidelines. As compared to non-infilled frames the AAC-infilled frames experienced a 20% reduction in inter-story drifts and a 25% increase in energy dissipation capacity as presented by Schwarz et al. [18]. This paper by Messaoudi et al. [19] investigates the in-plane seismic response of infilled RC frames using a strut modeling approach. The authors validate their simplified numerical model through experimental comparisons, achieving a maximum deviation of 23% for initial stiffness and 14% for maximum strength. The study highlights the effectiveness of optimized strut parameters in capturing the behavior of masonry-infilled frames, particularly in the presence of openings and varying infill strengths. The research emphasizes the importance of reliable numerical modeling in predicting seismic performance, addressing the complex interactions between infills and RC frames. These studies collectively emphasize the critical role of in-plane stiffness and absorption of dissipative forces in determining seismic performance of masonry filled reinforced concrete frames.

### 3. Research Methodology

The flow chart (Figure 1) shows the experimental investigation, analytical investigation by using structural analysis and design software's and analytical Investigation by using of AI tools.

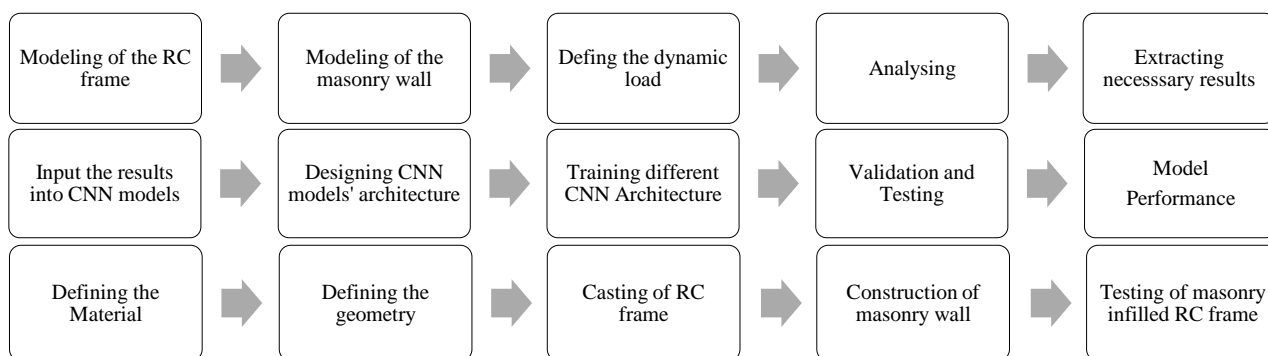


Figure 1. Flowchart of the methodology

#### 3.1. Specimen Preparation

The frame models used in the study are geometrically scaled down to half their original size, making the test specimens 1.5 m × 1.5 m compared to the actual 3 m × 3 m frame sizes used in the construction. Geometric scaling follows principles outlined in structural analysis and modeling texts, ensuring that the smaller models accurately replicate the behavior of their full-scale counterparts under similar loading conditions. The preparation of seven specimens involved constructing AAC block masonry walls within reinforced concrete frames. The M20 grade concrete is used for the casting of RC frames. The reinforcement consisted of Fe 250 and Fe 415 grade steel as presented in Table 1, with the diameter of bar as per the scaling law [19], ensuring the ductility and integrity of the frame under loading conditions.

Table 1. Frame reinforcement details

Member	Size [mm]	Top R/F [mm ϕ]	Bottom R/F	Stirrups
Bottom beam	160 × 185	2-10	3-10	6mm @ 35 [mm] c/c
Top beam	160 × 170	2-10	3-10	6mm @ 35 [mm] c/c
Member	Size [mm]	Main Steel		Ties
Column	160 × 170	4-10 mm		6mm @ 33 [mm] c/c

\* R/F-Reinforcement

For beams and columns, the sectional geometrical properties were calculated based on dimensional analysis, considering the scaled-down requirements while ensuring the structural characteristics matched those of the full-scale prototypes [19]. The design and construction of these frames adhered to the standard construction practices as specified in IS 456:2000 for concrete design, IS 13920:2016 for ductile detailing and IS 1893 (Part 1): 2016 for seismic design, ensuring that the specimens accurately replicated typical reinforced concrete structures used in seismic zones.

### 3.2. Testing Framework and Loading Protocol

The RC frames are mounted on a solid floor equipped with an MTS hydraulic actuator with a 100 kN capacity, featuring an inbuilt Linear Variable Differential Transformer (LVDT) for precise displacement measurements and a load cell for accurate force readings, to apply reverse cyclic loading to simulate seismic forces. The RC frame shown in Figure 2 is fixed between two rigid stoppers on the floor to prevent in-plane movement during the test.



Figure 2. Testing arrangement

A displacement control method is employed, applying cyclic loads at target displacements from 2 mm to 10 mm at 2 mm interval. This testing is performed across a range of frequencies from 1 Hz to 7 Hz, increasing in 1 Hz intervals. This setup ensures that the applied loads accurately reflect the dynamic behavior of RC frames under seismic conditions, enabling the assessment of the first and second secant stiffnesses.

## 4. Displacement Based Analysis

### 4.1. First and Second Secant Stiffness at 2 mm Displacement

The study of secant stiffnesses for masonry infilled reinforced concrete structure under cyclic loading at various frequencies from 1 Hz to 7 Hz shows significant variations in structural behavior, reflecting response of the frame to increasing lateral displacement and cyclic loads as shown in Figure 3. At 1 Hz, the first secant stiffness is 23.9% higher than the second, indicating initial stiffness degradation due to minor cracking and yielding at the frame-infill interface. As frequency increases to 2 Hz, the first secant stiffness drops sharply by 61.3%, suggesting severe initial damage, while the second secant stiffness shows a smaller reduction of 23.8%, indicating better energy dissipation in the second half-cycle.

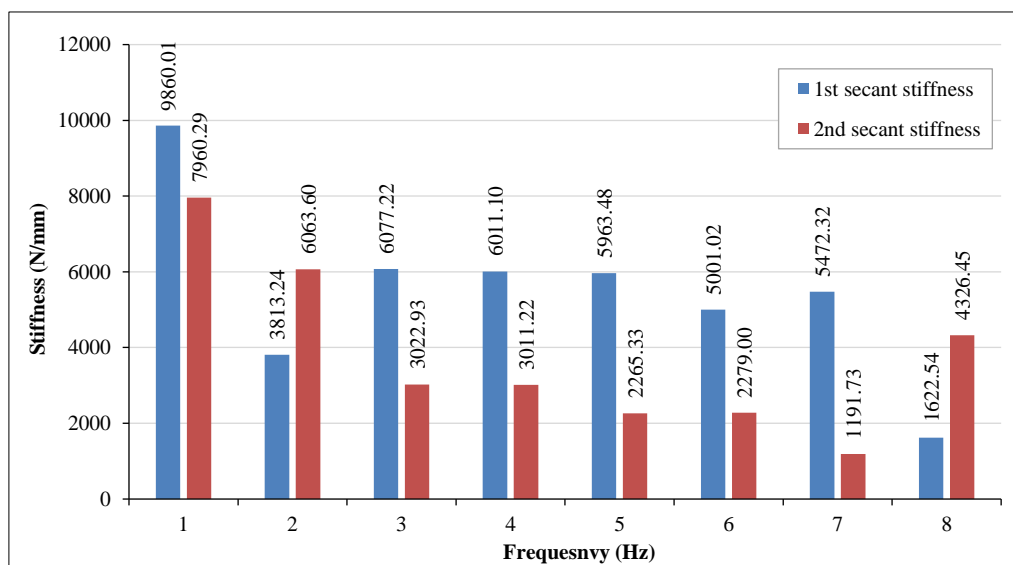


Figure 3. First and Second secant stiffness at 2 mm displacement

At higher frequencies like 3 Hz, there is a notable increase in the first secant stiffness by 59.3% due to improved frame-infill interaction. The second secant stiffness decreases by 50.1% which indicates cumulative damage along with decrease in energy dissipation capability. This behavior shows the accumulation of damage is accelerated at the increased loading frequency by making notable impact on energy dissipation as reported by Furtado et al. [4].

The damage accumulates further with decreased energy dissipation at a frequency of 5 Hz due to considerable reduction of 24.8% in second secant stiffness and a slight reduction of 0.8% in first secant stiffness. This trend continues with minor fluctuations at higher frequencies. A slight recovery in the first secant stiffness is observed at 7 Hz but the second secant stiffness experiences a sharp decline of 47.7% indicating significant cumulative damage in reverse direction of loading. The overall trend highlights the similar behaviour observed in previous studies [19].

#### 4.2. First and Second Secant Stiffness at 4 mm Displacement

The analysis of structure at 4 mm displacement and the frequency ranging from Hz to 7 Hz frequency presented in Figure 4 shows significant variations in first and second secant stiffness of masonry filled reinforced concrete frames under reverse cyclic loading.

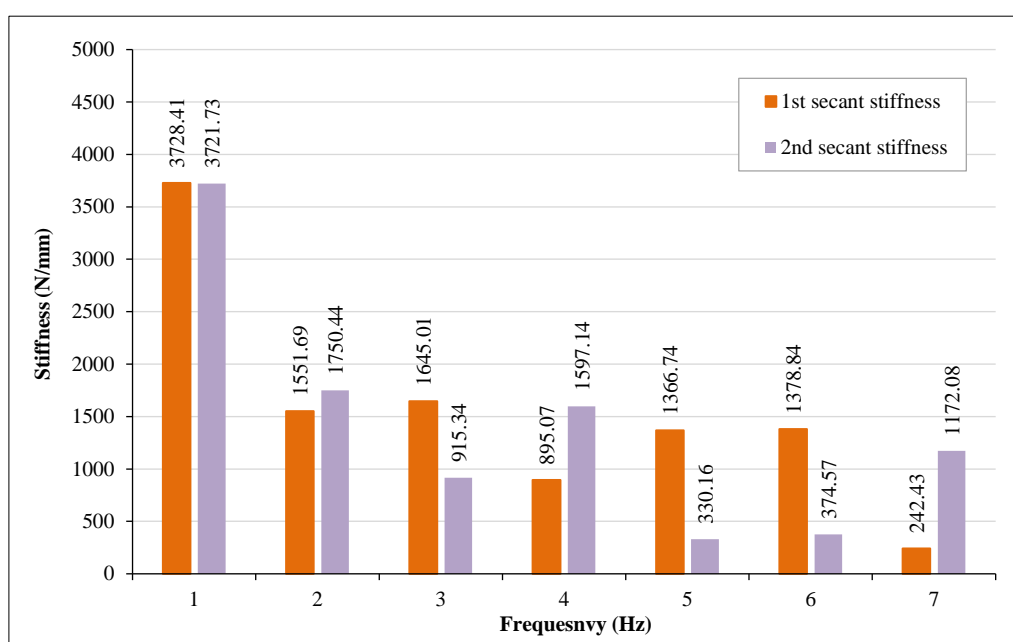


Figure 4. First and Second secant stiffness at 4 mm displacement

At 1 Hz, nearly identical stiffness values indicate minimal initial damage and strong frame-infill interaction, consistent with Xi & Liu [5], who observed that early-stage cyclic loading often preserves initial stiffness due to an intact frame-infill bond. As frequency increases to 2 Hz, a sharp reduction of 58.4% in the first secant stiffness and 53.0% in the second reflects initial cracking and yielding at the frame-infill interface, a sign to severe damage as noted by Harris & Sabnis [20]. At 3 Hz, the first secant stiffness shows a slight recovery 5.9%, likely due to temporary crack closure or redistribution of loads, whereas the second secant stiffness decreases by 47.7%, indicating cumulative damage, a pattern observed by Šipoš & Strukar [21]. At 4 Hz, the first secant stiffness drops by 45.6%, but the second increases by 74.5%, suggesting temporary stress redistribution and crack closure, aligning with Xi & Liu [5]. At 5 Hz, a 52.7% rise in first secant stiffness contrasts with a severe 79.3% drop in the second, pointing to significant damage and reduced energy dissipation, corroborating [22, 23]. At higher frequencies, 6 Hz and 7 Hz, minor changes in stiffness values indicate persistent degradation with minor stabilization. The first secant stiffness drops drastically by 82.4% at 7 Hz, while the second rises dramatically by 213%, signifying effective stress redistribution and crack stabilization in the later stages, supporting [5].

Figures 5-a and 5-b show the failure pattern. 1. At beam column joint shear cracks are observed (red). 2. AAC block has vertical crack, due to combination of vertical loads and horizontal loads (yellow). Stiffness variation plots show the higher rate of stiffness reduction which indicates unexpected damage after first crack appears [8].



Figure 5. Cracks in RC element and masonry block

### 4.3. First and Second Secant Stiffness at 6 mm Displacement

The analysis of first and second secant stiffness from 1 Hz to 7 Hz frequency at 6 mm displacement reveals significant variations in the response of masonry filled reinforced concrete frames under cyclic loading, as shown in Figure 6.

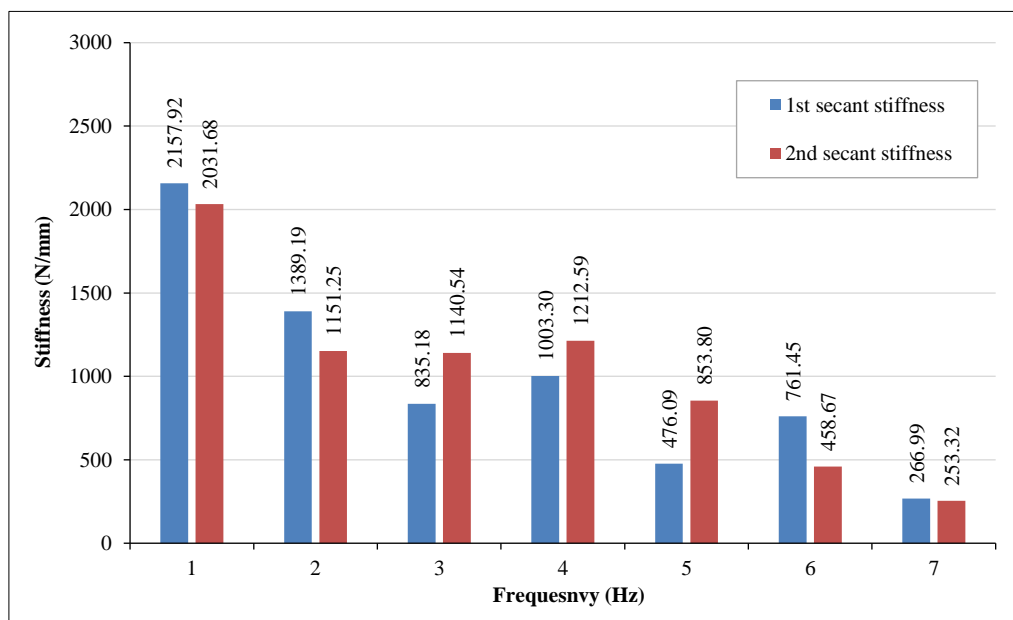


Figure 6. First and Second secant stiffness at 6 mm displacement

The analysis of first and second secant stiffness at 6 mm displacement from 1 Hz to 7 Hz frequency reveals substantial stiffness degradation and progressive structural damage in AAC masonry wall filled concrete frames for cyclic loading test. At 1 Hz, first secant stiffness is only 9% higher than the second, indicating minor initial damage due to early-stage cracking. As frequency increases to 2 Hz, a sharp reduction of 27.6% and 32.5% in the first and second secant stiffness, respectively, signals severe damage and yielding of stirrups, as observed by Wang [11]. This trend continues at 3 Hz with further reductions of 15.5% and 23.8%, reflecting a significant compromise in load-bearing capacity and energy dissipation. At 4 Hz, the reductions stabilize to around 12.4% and 13.4%, suggesting a shift towards a more stable but still degraded state, marked by plastic hinge formation and stress redistribution. At 5 Hz, further decreases of 12.3% and 15.5% indicate extensive damage and weakening of the frame-infill bond. By 6 Hz, the system shows signs of minor stabilization with a 5.5% drop in the first and 13.8% in the second secant stiffness, but the continued yielding and crack propagation suggest nearing inelastic capacity limits. At 7 Hz, severe damage is evident with reductions of 12% and 17.9%, indicating multiple plastic hinges and a diminished ability to resist seismic forces.

### 4.4. Hysteresis Behavior of Load vs. Displacement

The interaction between the RC frame and masonry infill plays a pivotal role in dictating structural behavior, particularly in terms of stiffness degradation and energy dissipation, as observed in recent studies [19, 24, 25]. At 4 mm lateral displacement and 2 Hz frequency the energy dissipation pattern is asymmetrical with 62.71% of the total energy

dissipated in the first half-cycle and only 37.29% in the second (Figure 7). This suggests greater inelastic deformation and damage accumulation during the initial loading phase consistent with findings by Shah et al. [24] on the role of frame-infill interaction in energy dissipation. The Bouc–Wen hysteresis model, known for its ability to capture gradual stiffness degradation and pinching effects, could be instrumental in numerically replicating this behavior. By incorporating parameters for energy dissipation asymmetry and inelastic deformation the model offers a refined representation of the hysteretic response [25]. The hysteresis loops exhibit a 12.82% increase in reloading stiffness from the first to the second half-cycle reflecting a temporary stiffening effect. This phenomenon can be attributed to combined resistance from the RC frame and partially damaged masonry wall during load reversal. These trends align with the refined strut modeling approach validated by Messaoudi et al. [19] demonstrates how reloading stiffness trends under cyclic loading provide critical insights into frame behavior. In this context, the Bouc–Wen model's pinching and degradation parameters can effectively replicate the observed increase in reloading stiffness. These parameters account for the stiffness recovery due to load reversals and provide an improved understanding of the dynamic response. The structure demonstrates compliance with IS 1893:2016 by achieving 59.55% and 57.88% of the maximum allowable displacement during the first and second half-cycles, respectively. The Bouc–Wen model is particularly advantageous in validating such compliance by enabling the evaluation of residual displacements and permanent deformations. Its application allows research for enhanced prediction of the structural response under cyclic and seismic loading conditions, particularly when combined with experimentally validated models like those in Messaoudi et al. [19].

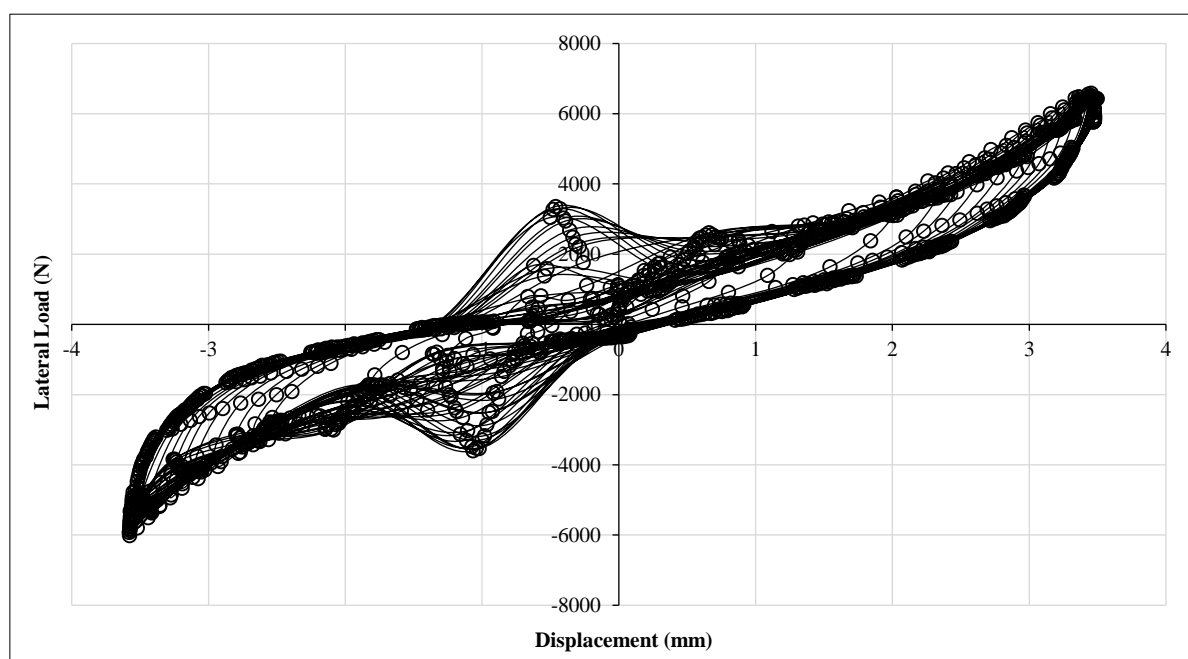


Figure 7. Hysteresis plot of load vs displacement at 4 mm displacement

#### 4.5. Summary of the Displacement based Response

Significant variations in secant stiffness at 2 mm displacement reflect the structure's elastic response, with reductions reaching 61.3% at 2 Hz frequency, as noted by Van & Lau [27]. At 4 mm displacement, the degradation becomes pronounced, driven by flexural-shear interaction and diagonal cracking in the masonry infill. Teguh [28] corroborates this by identifying similar stiffness reductions linked to extensive cracking and bond-slip effects in infilled RC frames. The consistent degradation of the first secant stiffness across frequencies, exceeding 50%, indicates progressive damage and the onset of plastic hinges, a phenomenon also observed in Teguh's experimental investigations. The hysteresis loops exhibit distinct pinching behavior, indicative of bond-slip effects and cumulative cracking at the frame-infill interface. This aligns with findings by Shah et al. [24] and Teguh [28], where pinching was linked to reduced stiffness and constrained energy dissipation. The asymmetric energy dissipation pattern, with more energy absorbed during the initial half-cycle than the subsequent one, reflects inelastic deformations and damage accumulation, as discussed in both studies. At higher displacement amplitudes, the progressive damage corresponds to the formation of plastic hinges and severe cracking patterns, as observed in both Van & Lau [27] and Teguh [28]. The failure modes include diagonal shear cracking, separation at the frame-infill interface and localized crushing in masonry, illustrating the composite action and interaction between the RC frame and the infill. The hysteresis behavior underscores the necessity of incorporating advanced analytical models to capture the complex interactions in masonry infilled RC frames. Models such as the Bouc–Wen hysteresis model, validated by Shah et al. [24] and Teguh [28], effectively simulate nonlinearities, pinching effects, and stiffness degradation. These models are critical for predicting structural performance under seismic conditions and guiding design improvements.

## 5. Frequency Based Analysis

### 5.1. First and Second Secant Stiffness at 1 Hz Frequency

At 2 mm displacement, the initial first secant stiffness is 19.3% higher than the second, reflecting early stiffness degradation due to minor cracks and yielding at the frame-infill interface. This initial loss indicates strong interaction but with minor initial damage due to the development of gaps. As the displacement increases to 4 mm, the first secant stiffness reduces by 62.2% and the second by 53.3%, as shown in Figure 8, demonstrates significant initial damage. The minimal difference between the two secant stiffness values (0.2%) suggests that the system has stabilized despite extensive damage, maintaining comparable energy dissipation in both half-cycles.

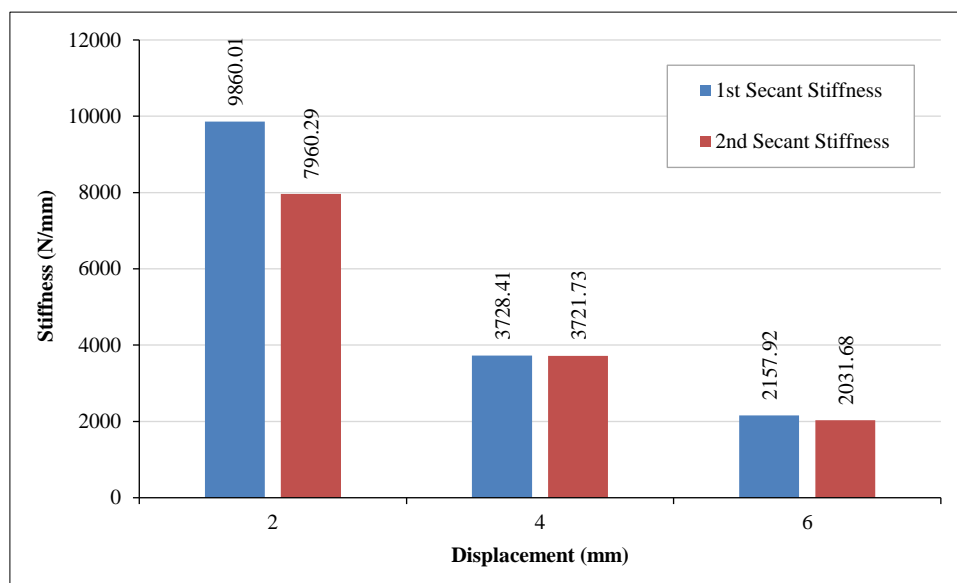


Figure 8. First and Second secant stiffness at 1 Hz frequency

At 6 mm displacement, the first secant stiffness decreases by 42.1% and the second by 45.4%, indicating progressive degradation and the development of plastic hinges. Figure 6 presents the first and second secant stiffness of concrete frame filled with AAC block masonry under cyclical loading at 1 Hz frequency.

Overall, the structural response reveals a pattern of initial stiffness loss due to cracks and minor yielding, followed by significant damage at 4 mm due to flexure-shear interaction and diagonal extrusion of the masonry. As displacement increases, the formation of plastic hinges and yielding of stirrups become more pronounced, reducing the frame's capacity to dissipate energy.

### 5.2. First and Second Secant Stiffness at 2 Hz Frequency

Figure 9 presents the first and second secant stiffness of frame composed of beam and column along with AAC block masonry at 2 Hz frequency. The structural behavior of the RC frame with AAC infill under cyclic loading shows significant variations in stiffness across different displacement levels. At 2 mm displacement, the first secant stiffness is 59% lower than the second secant stiffness, indicating early damage stabilization and improved activeness of the masonry wall within the frame of concrete beam and column in second half cycle. As the displacement increases to 4 mm, both stiffness values show a sharp decline, with the first secant stiffness reducing by 59.3% and the second secant stiffness by 71.1% from their initial values. This indicates severe initial damage due to diagonal cracks and yielding, though the second half cycle still shows slightly better energy dissipation.

At 6 mm displacement, the reduction in the first secant stiffness slows down to 10.5%, while the second secant stiffness drops significantly by 34.3%, reflecting the progression of damage and a decrease in the frame's capacity to resist further deformation. The reduction in stiffness at this stage suggests that cumulative damage and plastic hinge formation are affecting the structural integrity, reducing the effectiveness of energy dissipation mechanisms.

Overall, the structural response under 2 Hz cyclic loading demonstrates that initial cracks and yielding at lower displacements lead to progressive degradation as displacement increases. The RC frame initially stabilizes after initial damage, but as the displacement grows, the system's load-deflection response and dissipative capabilities decline because of flexure-shear damage and plastic hinge formation, particularly in the second half cycle of loading.

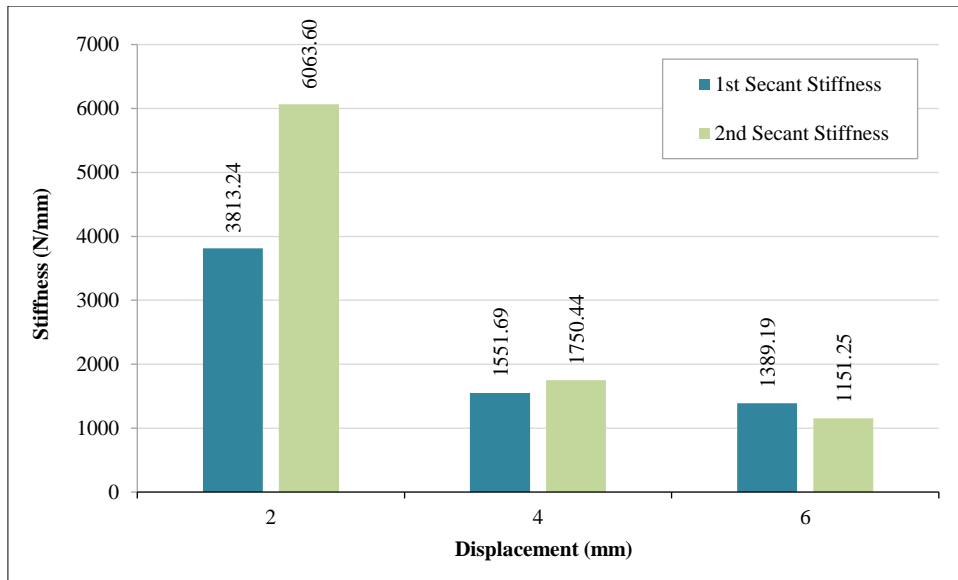


Figure 9. First and Second secant stiffness at 2 Hz frequency

**5.3. First and Second Secant Stiffness at 3 Hz Frequency**

Figure 10 represents the first and second secant stiffness of the frame-wall assembly under cyclic loading at 3 Hz frequency.

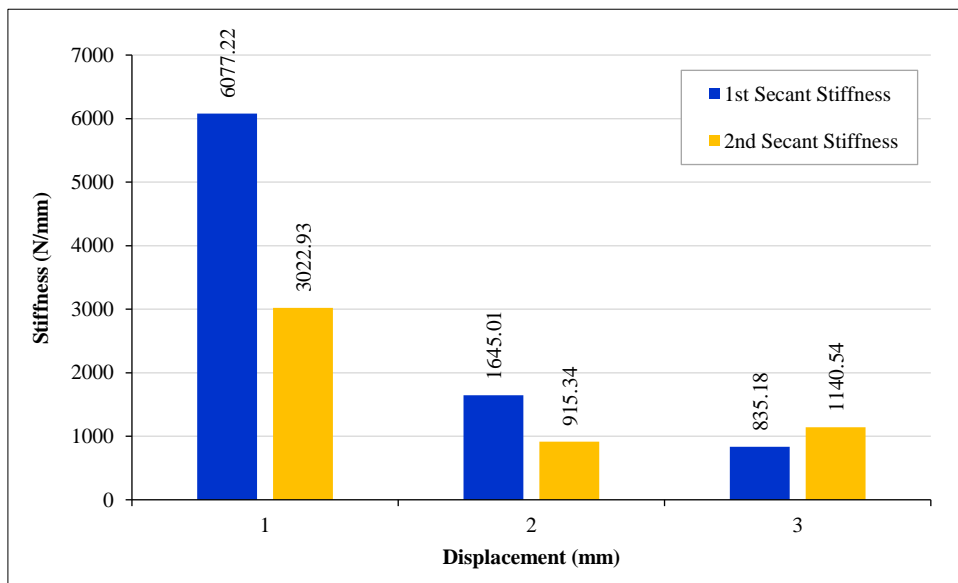


Figure 10. First and Second secant stiffness at 3 Hz frequency

The data shows that the first secant stiffness significantly decreases with increasing displacement, with a 50.2% reduction between 2 mm and 4 mm, followed by another 49.2% reduction at 6 mm displacement. The second secant stiffness also declines, with a 69.7% decrease from 2 mm to 4 mm and an 8.7% reduction from 4 mm to 6 mm. This pattern indicates progressive damage accumulation, which is characterized by pronounced flexural-shear interaction and yielding of the reinforcement.

At lower displacements (2 mm), the homogeneous resistance among the masonry and beam column frame unit results in high initial stiffness. Due to minor cracks and localized yielding stiffness in the second half-cycle reduces, aligning with the findings in the referenced study, where initial damage is marked by shear cracks and diagonal cracking. At higher displacements (4 mm and 6 mm), the sharp reduction in stiffness highlights increased diagonal extrusion of masonry and extensive cracking, likely leading to gaps between the AAC infill and RC frame. This is further compounded by flexural-shear failures due to loss in shear strength at masonry joints and diagonal compression of the masonry. The energy absorbed through inelastic deformations increases when frame-infill interaction weakens, confirming the findings on enhanced lateral ductility and stiffness degradation under cyclic loads as noted in the study.

### 5.4. First and Second Secant Stiffness at 4 Hz Frequency

The bar chart presents the first and second secant stiffness of entire frame-wall unit for cyclic loading test at 4 Hz frequency, as shown in Figure 11. At 4 Hz frequency, the first secant stiffness drops sharply from 6011.10 N/mm at 2 mm displacement to 1597.14 N/mm at 4 mm, showing a 73.4% reduction. The second secant stiffness also decreases significantly, from 3022.93 N/mm to 915.34 N/mm, reflecting a 69.7% decline. At 6 mm displacement, the first secant stiffness reduces further by 24.1%, reaching 1212.59 N/mm, while the second secant stiffness unexpectedly increases by 24.6% to 1140.54 N/mm, indicating partial stabilization. The marked reduction in stiffness at lower displacements is due to early flexural-shear interaction and localized yielding. The continued decrease with increasing displacement signifies progressive damage, with plastic hinges forming at critical sections, reducing the load-bearing capacity. The temporary recovery at higher displacements suggests some stress redistribution, but the overall energy dissipation capacity remains compromised, consistent with the behavior observed in cyclic loading test.

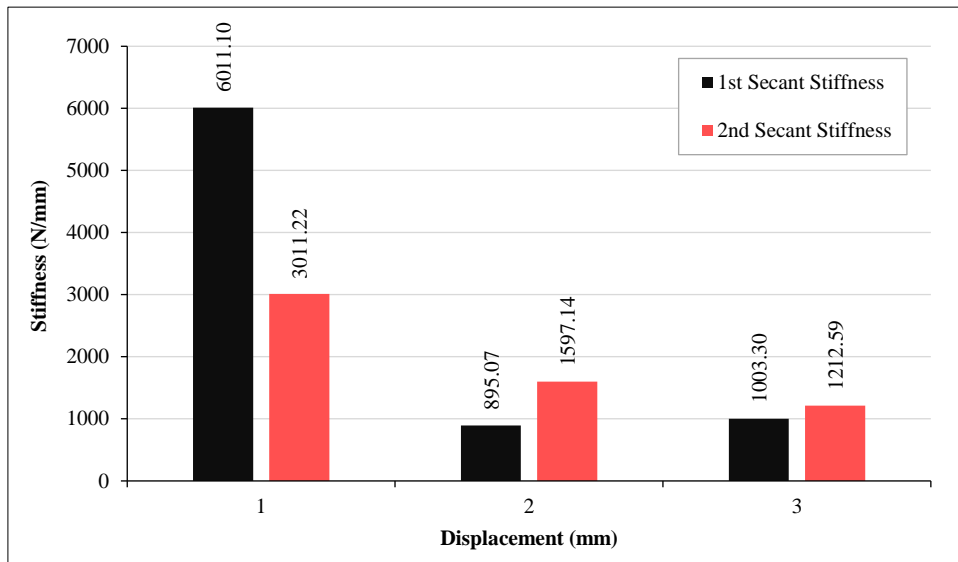


Figure 11. First and Second secant stiffness at 4 Hz frequency

### 5.5. First and Second Secant Stiffness at 5 Hz Frequency

At 2 mm displacement, the first secant stiffness is 55.3% higher than the second secant stiffness. At 4 mm, the first secant stiffness reduces by 73.0% compared to 2 mm, while the second secant stiffness shows an 85.4% reduction from the previous 2 mm value, as shown in Figure 12. At 6 mm displacement, the first secant stiffness drops further by 65.2% from 4 mm, while the second secant stiffness increases by 158.6% from 4 mm. This variation suggests significant degradation and partial recovery in energy dissipation capacity at higher displacements. The high initial stiffness at 2 mm suggests strong takeover among the frame and masonry wall. The significant drop in second secant stiffness indicates minor cracking and slight deformation of the RC frame.

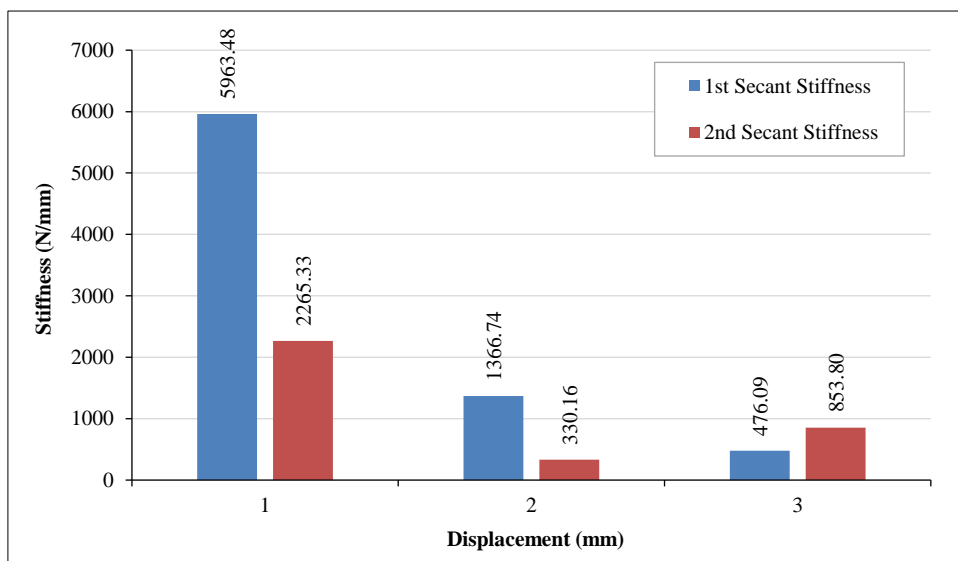


Figure 12. First and Second secant stiffness at 5 Hz frequency

At 4 mm, the sharp decline in stiffness values reflects extensive damage, with possible diagonal extrusion of masonry and the opening of gaps at the frame-infill interface. At 6 mm, the further reduction in first secant stiffness, coupled with an increase in the second secant stiffness, suggests partial stabilization. This behavior indicates generation of inelastic hinges and stress redistribution within the frame, allowing for enhanced energy dissipation in the later half-cycle despite severe flexural-shear interaction.

**5.6. First and Second Secant Stiffness at 6 Hz Frequency**

At 6 Hz frequency, the first secant stiffness shows a reduction of 55% from 5001.02 N/mm at 2 mm to 2279.00 N/mm at 4 mm displacement, as shown in Figure 13. A further decrease of 39.5% is observed from 4 mm to 6 mm displacement. The second secant stiffness follows a more pronounced decline, with a 54% drop from 2279.00 N/mm at 2 mm to 374.57 N/mm at 4 mm and a 40.8% reduction from 4 mm to 6 mm displacement. This trend signifies progressive degradation of the frame-infill wall assembly, primarily caused by cumulative inelastic displacements and damage propagation in the masonry. Structurally, the reduction in stiffness with increased displacement indicates severe deformation, likely involving diagonal cracking, extrusion of masonry and wall-frame gaps. The lower second secant stiffness reflects diminished energy dissipation capacity, likely due to yielding of reinforcement and formation of plastic hinges at critical sections, weakening the frame's ability to resist cyclic loads effectively.

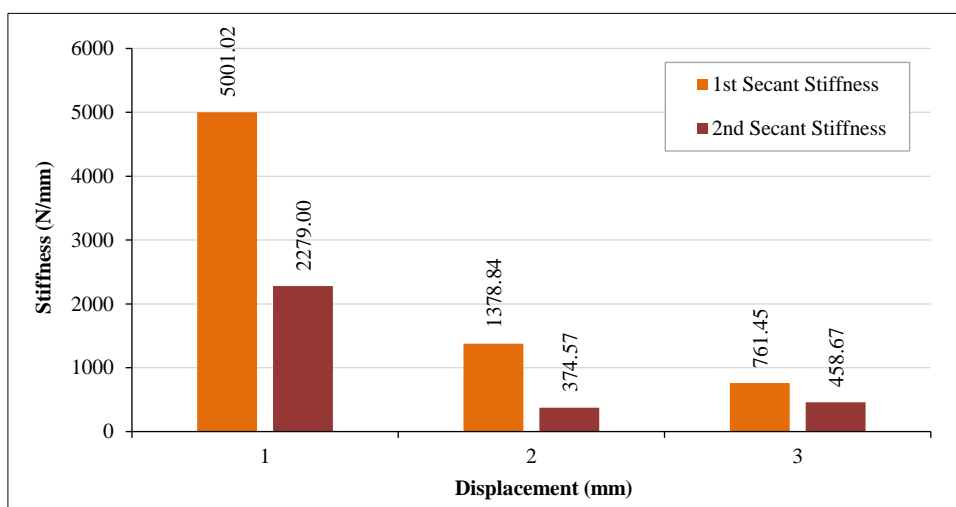


Figure 13. First and Second secant stiffness at 6 Hz frequency

**5.7. First and Second Secant Stiffness at 7 Hz Frequency**

For the frequency-controlled testing at 7 Hz, the first secant stiffness experiences a substantial drop, indicating severe degradation, as shown in Figure 14. At 2 mm displacement, the first secant stiffness is 5472.32 N/mm, which decreases sharply to 242.43 N/mm at 4 mm displacement, a reduction of 95.6%. The second secant stiffness, however, shows a less drastic decline of 3.2% from 1191.73 N/mm at 2 mm to 1172.08 N/mm at 4 mm. The first secant stiffness slightly increases by 10.1% to 266.99 N/mm at 6 mm, while the second secant stiffness decreases by 78.4% to 253.32 N/mm from the previous value at 4 mm. This behavior illustrates significant energy dissipation and stiffness loss in the frame, especially during the initial cycles, which is consistent with observations at this frequency.

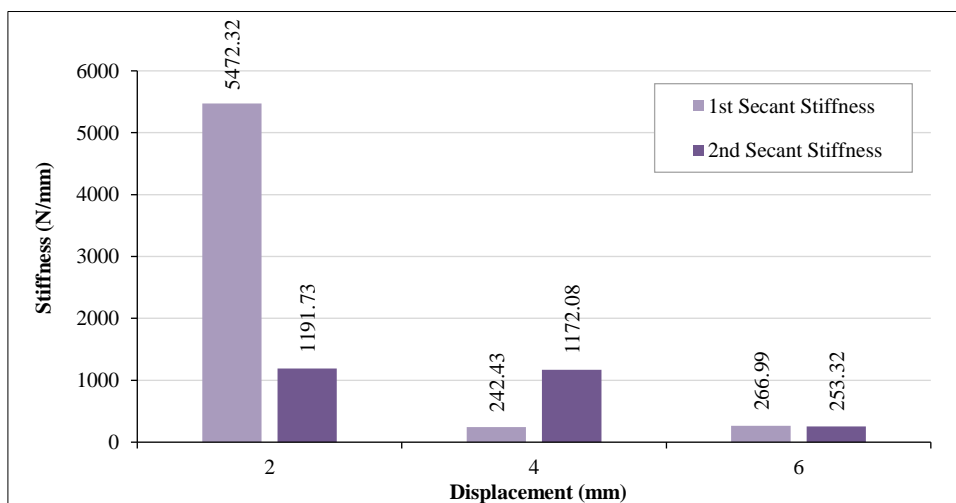


Figure 14. First and Second secant stiffness at 7 Hz frequency

The substantial reduction in first secant stiffness is indicative of severe deformation and progressive damage in the frame and significant diagonal extrusion within the masonry wall. The decreasing trend and variations in the second secant stiffness highlight the structure's reduced capacity to absorb energy in subsequent cycles, as reported by Cavaleri et al. [29]. This suggests that at higher frequencies, the frame experiences distinct flexure-shear behavior and potential plastic hinge formation, leading to considerable decrease in lateral movement and overall energy dissipation capacity.

### 5.8. Hysteresis Behavior of Load vs. Displacement

The hysteresis loops demonstrate pronounced pinching behavior as illustrated in Figure 15 especially at lower displacement amplitudes. This behavior is consistent with findings by Shah et al. [24] which have attributed to the friction and sliding at the frame-infill interface as well as the progressive deterioration of the masonry. Pinching leads to a 35–40% reduction in loop width reflecting reduced stiffness and energy dissipation capacity. The initial secant stiffness representing the steep gradient of the first cycles was moderated by 25–30% in subsequent cycles by correlating with progressive separation cracks at the frame-infill interface and the development of diagonal cracks within the masonry wall. Such degradation aligns with Shah et al.'s observations of stiffness loss due to bond failures and infill-frame interaction effects. The energy dissipation capacity also exhibited a significant decline with the hysteresis loop area decreasing by 30–35% in successive cycles. This reduction underscores the reduced ability of the structure to absorb and dissipate seismic energy primarily due to the widening of cracks and loss of friction at the frame-infill interface. The hysteresis response displayed 10–15% asymmetry in the maximum lateral loads between positive and negative directions indicating non-uniform damage within the infill and frame elements.

At higher displacement amplitude the load-carrying capacity declined by 20–25% demonstrating inelastic deformation and substantial damage to both the masonry and RC frame. Residual deformation reached 10–12% of the maximum displacement emphasizing the inelastic nature of the response and permanent damage accumulation [30]. The findings closely align with Su et al. [31] who observed that infilled RC frames demonstrate enhanced initial stiffness and energy dissipation compared to bare frames but suffer rapid degradation under cyclic loading. The study noted that the energy dissipation capacity of infilled frames was 2.3 times higher than bare frames initially but decreased significantly as damage accumulated. Similar pinching behavior and stiffness degradation were attributed to diagonal cracking and corner crushing in the masonry. The observed hysteresis behavior highlights the critical influence of frame-infill interaction on seismic performance. The degradation of stiffness and energy dissipation capacity coupled with residual deformations and load asymmetry necessitates the incorporation of reduced secant stiffness in seismic assessment methodologies.

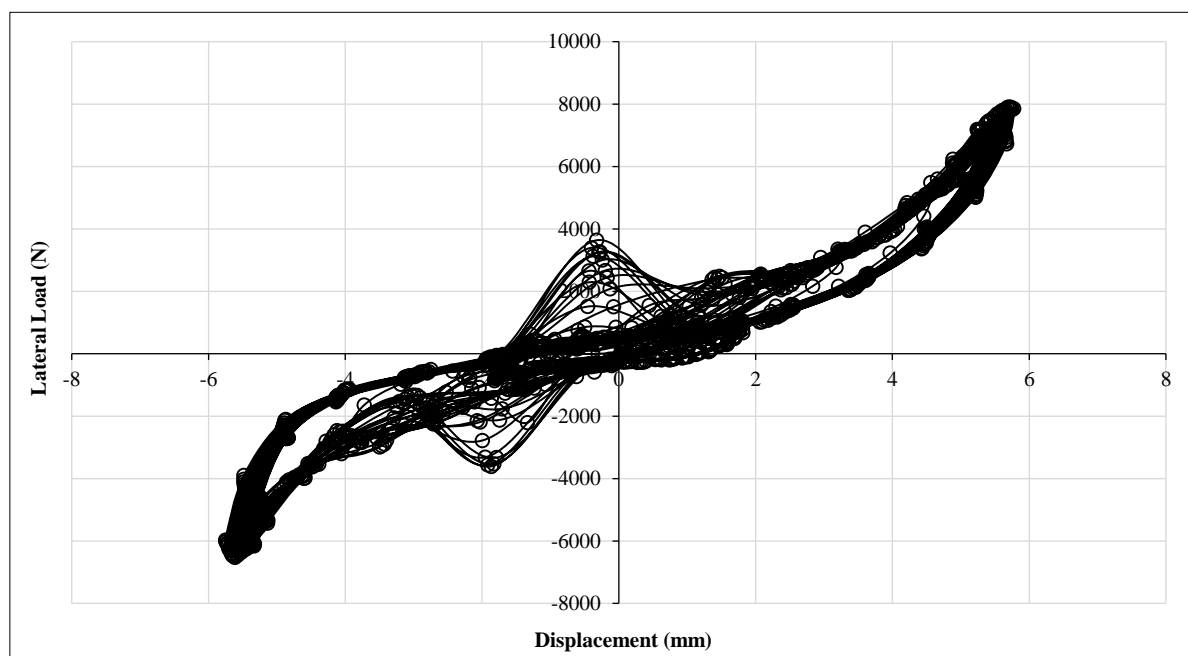


Figure 15. Hysteresis plot of load vs displacement at 6 mm displacement

### 5.9. Summary of Frequency Based Investigation

The cyclic behavior of AAC block masonry infilled RC frames demonstrate significant sensitivity to displacement amplitude and frequency, with progressive stiffness degradation and structural damage consistent with reported trends for masonry infilled frames under lateral loading [24, 26]. At lower frequencies (1 Hz), the initial damage is minimal

with the first secant stiffness at 2 mm displacement showing a 19.3% increase compared to degraded states. However, at 4 mm displacement, the stiffness reduces sharply by 62.2% due to diagonal cracking of the masonry and yielding of stirrups within the RC frame. These findings are consistent with the lateral stiffness reduction mechanisms [26]. As the loading frequency increases to 2 Hz, the first secant stiffness decreases by 59% at 2 mm with plastic hinges forming near beam-column joints as displacement increases as shown in Figure 16.



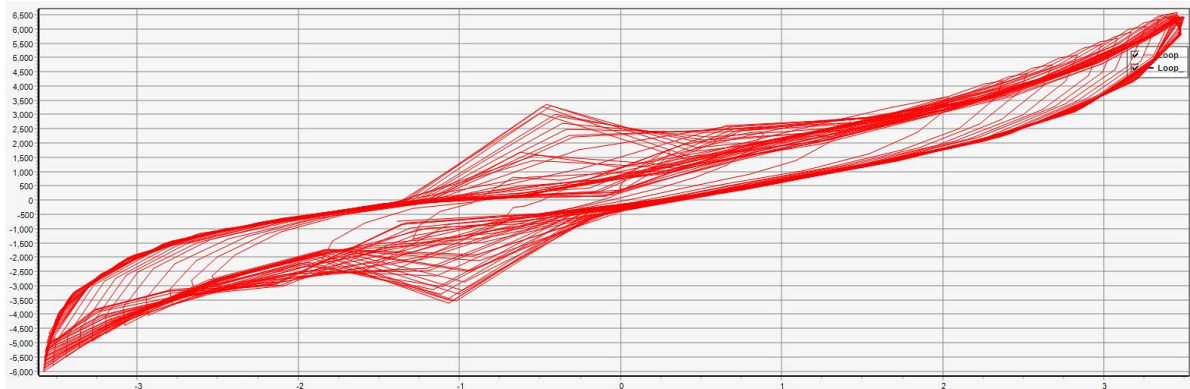
**Figure 16. Cracks at beam-column joint**

This rapid stiffness decline is indicative of bond degradation and stress redistribution supported by the hysteretic energy dissipation trends in Shah et al. [24]. At 3 Hz, a consistent 50% reduction in stiffness reflects the cumulative damage and weakening of the infill-frame bond. Higher frequencies (4-5 Hz) induce more severe damage, with the first secant stiffness reducing by 73.4% between 2 mm and 4 mm displacement and an additional 24.1% drop at 6 mm displacement. These reductions highlight the development of extensive cracking and stress redistribution in the frame and infill. At 6 Hz, stiffness decreases by 55% at 2 mm and 39.5% at 4 mm, indicating substantial deformation, reduced energy dissipation and yielding of reinforcement elements. Such frequency-dependent degradation patterns on the pivotal role of interface behavior and dynamic effects in cyclic loading [26]. At 7 Hz, the behavior becomes critically unstable, with the first secant stiffness dropping by a staggering 95.6% at 4 mm displacement. The second secant stiffness shows a 78.4% reduction, underscoring severe structural damage and limited residual capacity. This drastic decline is a hallmark of advanced plasticity, localized crushing and loss of lateral load resistance, paralleling the hysteretic collapse modes discussed in Shah et al. [24]. The pronounced degradation in stiffness and energy dissipation capacity observed under increasing frequency highlights the need for dynamic models that incorporate frequency-dependent stiffness degradation, bond-slip effects and energy dissipation mechanisms. The cyclic response of AAC block masonry infilled RC frames underscore the critical interplay between frequency, displacement amplitude and stiffness degradation.

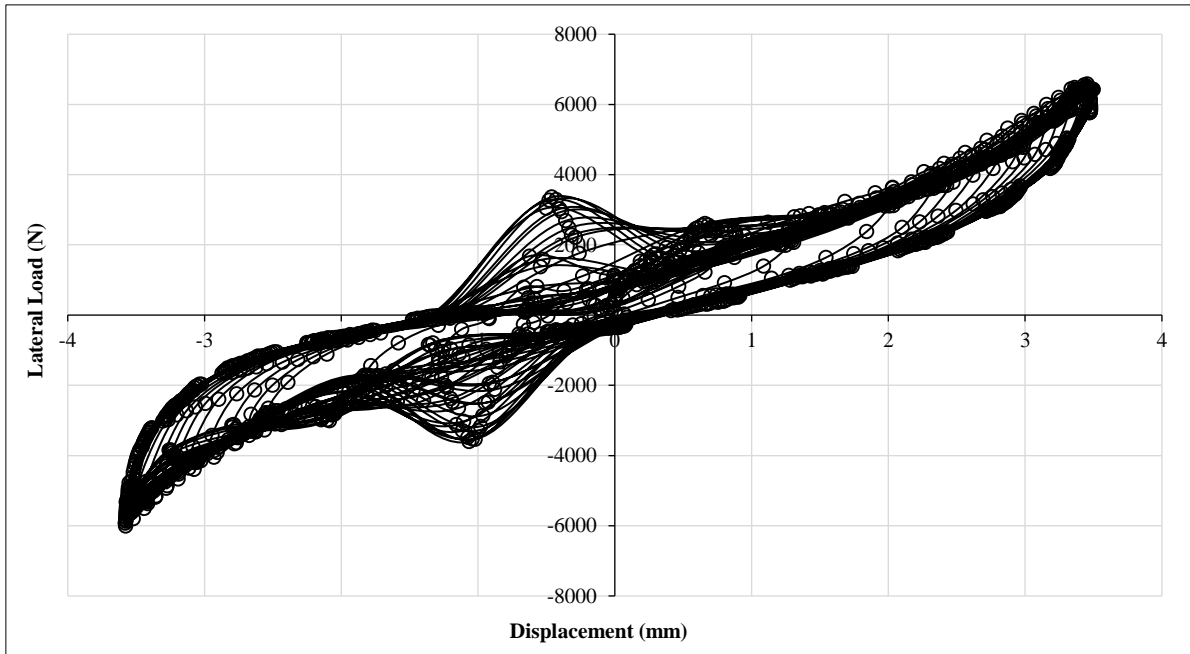
## **6. Application of AI Driven Tools for Prediction of Hysteresis Loop**

This study addresses gaps in literature by focusing on the first and second secant stiffness degradation under varying frequency and displacement conditions, particularly for AAC masonry infills. Additionally, the use of AI techniques, i.e. LSTM-CNNs for predictive modeling represents a novel approach, as most existing studies rely on traditional experimental and analytical methods.

The predictive workflow begins with Data Representation and Preprocessing, where features like frequency, energy dissipation, and secant stiffness are normalized using MinMaxScaler and reshaped into a 3D format suitable for sequential analysis. This step ensures that the data is ready for efficient processing by neural networks while retaining spatial and temporal relationships. The model integrates a Convolutional Neural Network (CNN) to extract spatial features, followed by a Long Short-Term Memory (LSTM) module that captures temporal dependencies in the data. An Attention Layer enhances the LSTM's focus on critical features, improving prediction accuracy. The outputs of the CNN and LSTM are combined in a unified representation, processed by fully connected layers with dropout regularization to prevent overfitting. The predicted plots for 4 mm displacement at 2 Hz frequency are shown in Figure 17-a and the experimental plot is shown in Figure 17-b.



(a) Predicted plot



(b) Experimental plot

Figure 17. Comparative plots of hysteresis loop

This hybrid CNN-LSTM architecture effectively captures both spatial and temporal patterns, enabling accurate predictions of seismic behavior.

### 7. Conclusions

The following results are derived from the experimental and analytical research done on the masonry infilled RC frame:

- At 1 Hz, the first secant stiffness is 19.3% higher than the second secant stiffness, indicating early-stage stiffness degradation due to minor cracking and bond-slip at interfaces. By 5 Hz, both stiffnesses experience significant reductions (73.0% for the first and 85.4% for the second), highlighting the increasing vulnerability of the masonry-infilled RC frame to frequency-induced cyclic loading.
- At 6 Hz and 7 Hz, the second secant stiffness drops by up to 78.4%, reflecting severe damage accumulation and diminished energy dissipation capacity. This suggests a critical threshold where the frame transitions into inelastic behavior, with structural elements entering advanced damage states.
- Plastic hinge formation is evident at frequencies above 5 Hz, with stiffness reductions exceeding 50%, leading to cumulative damage and significant loss of load-bearing capacity. The increased hysteretic energy dissipation during these cycles highlights the need for advanced retrofitting techniques to mitigate such losses under dynamic loading.
- At 2 mm displacement, the first secant stiffness remains consistently higher across all frequencies, indicating robust elastic behavior and strong frame-infill interaction. However, at 4 mm displacement, sharp declines in stiffness highlight early damage initiation, with cracking and bond-slip becoming more pronounced.

- Between 4 mm and 6 mm displacement, both stiffnesses show consistent reductions across frequencies, with prominent flexure-shear interactions and plastic hinge formation, particularly at 3 Hz. This behavior underscores the influence of displacement amplitude on the progression of cumulative damage and degradation.
- At 6 mm displacement, minor improvements in the second secant stiffness (e.g., 0.6% at 6 Hz) suggest temporary stress redistribution due to crack bridging and localized material hardening. However, cumulative reductions of up to 39.5% in first secant stiffness and 40.8% in second secant stiffness indicate progressive degradation and declining structural integrity under larger cyclic loads.

This research underscores the critical impact of loading frequency and displacement on the reduction in load vs deformation capabilities along with considerable energy dissipation of RC beam column frame filled with masonry unit. Overall, there is the need for incorporating advanced stiffness degradation models into seismic design frameworks because of distinct stiffness reduction at higher frequencies and displacements indicates

## 8. Declarations

### 8.1. Author Contributions

Conceptualization, A.A.G.; methodology, A.A.G. and S.B.P.; formal analysis, S.B.P.; investigation, A.A.G. and S.B.P.; data curation, A.A.G.; writing—original draft preparation, A.A.G.; writing—review and editing, A.A.G. and S.B.P.; supervision, S.B.P. All authors have read and agreed to the published version of the manuscript.

### 8.2. Data Availability Statement

The data presented in this study are available on request from the corresponding author.

### 8.3. Funding

The authors received no financial support for the research, authorship, and/or publication of this article.

### 8.4. Conflicts of Interest

The authors declare no conflict of interest.

## 9. References

- [1] Xi, K., & Liu, B. (2022). Seismic Performance and Finite Element Analysis of Reinforced Concrete Frames Considering a Masonry-Infilled Wall. *Advances in Materials Science and Engineering*, 2022, 6832624. doi:10.1155/2022/6832624.
- [2] Raj, P., & Ravula, M. B. (2022). Experimental Investigation on Mechanical Behavior of AAC Block Masonry. *IOP Conference Series: Materials Science and Engineering*, 1255(1), 012016. doi:10.1088/1757-899x/1255/1/012016.
- [3] Zade, N. P., Bhosale, A., Sarkar, P., & Davis, R. (2022). In-Plane Seismic Response of Autoclaved Aerated Concrete Block Masonry-Infilled Reinforced Concrete Frame Building. *ACI Structural Journal*, 119(2), 45–60. doi:10.14359/51734329.
- [4] Furtado, A., Rodrigues, H., & Arêde, A. (2022). Effect of the Openings on the Seismic Response of an Infilled Reinforced Concrete Structure. *Buildings*, 12(11), 20. doi:10.3390/buildings12112020.
- [5] Đorđević, F., & Marinković, M. (2024). Advanced ANN Regularization-Based Algorithm for Prediction of the Fundamental Period of Masonry Infilled RC Frames. *Journal of Big Data*, 11, 169. doi:10.1186/s40537-024-01027-z.
- [6] Sullivan, T. J., Calvi, G. M., & Priestley, M. J. N. (2004, August). Initial stiffness versus secant stiffness in displacement based design. *13<sup>th</sup> World Conference of Earthquake Engineering (WCEE)*, 1-6 August 2004, Vancouver, Canada.
- [7] Gaikwad, N. C., Galatage, A. A., & Kulkarni, S. K. (2017). Scaling Of Ground Motions for Performing Incremental Dynamic Analysis of RC Framed Structures. *International Journal of Advance Research, Ideas and Innovations in Technology*, 3(5), 56–68.
- [8] Sivanantham, P., Selvan, S. S., Srinivasan, S. K., Gurupatham, B. G. A., & Roy, K. (2023). Influence of Infill on Reinforced Concrete Frame Resting on Slopes under Lateral Loading. *Buildings*, 13(2), 289. doi:10.3390/buildings13020289.
- [9] Thisovithan, P., Aththanayake, H., Meddage, D. P. P., Ekanayake, I. U., & Rathnayake, U. (2023). A novel explainable AI-based approach to estimate the natural period of vibration of masonry infill reinforced concrete frame structures using different machine learning techniques. *Results in Engineering*, 19, 101388. doi:10.1016/j.rineng.2023.101388.
- [10] Cattari, S., Calderoni, B., Calì, I., Camata, G., de Miranda, S., Magenes, G., ... & Saetta, A. (2022). Nonlinear modeling of the seismic response of masonry structures: critical review and open issues towards engineering practice. *Bulletin of Earthquake Engineering*, 20(4), 1939-1997. doi:10.1007/s10518-021-01263-1.

- [11] Wang, F. (2023). Experimental Research on Seismic Performance of Masonry-Infilled RC Frames Retrofitted by Using Fabric-Reinforced Cementitious Matrix under In-Plane Cyclic Loading. *International Journal of Concrete Structures and Materials*, 17(1), 31. doi:10.1186/s40069-023-00594-4.
- [12] Blasi, G., De Luca, F., & Aiello, M. A. (2018). Brittle failure in RC masonry infilled frames: The role of infill overstrength. *Engineering Structures*, 177, 506–518. doi:10.1016/j.engstruct.2018.09.079.
- [13] Cai, G., & Su, Q. (2019). Effect of Infills on Seismic Performance of Reinforced Concrete Frame structures—A Full-Scale Experimental Study. *Journal of Earthquake Engineering*, 23(9), 1531–1559. doi:10.1080/13632469.2017.1387194.
- [14] Chen, H., & Bai, J. (2021). Seismic performance evaluation of buckling-restrained braced RC frames considering stiffness and strength requirements and low-cycle fatigue behaviors. *Engineering Structures*, 239, 112359. doi:10.1016/j.engstruct.2021.112359.
- [15] Kurmi, P.L., Kumar, N., & Telang, D. (2024). Effect of Infills with Realistic Openings on the Seismic Performance of Gravity Load-Designed RC Buildings. *Technologies for Sustainable Buildings and Infrastructure, SIIOC 2023, Lecture Notes in Civil Engineering*, 528, Springer, Singapore. doi:10.1007/978-981-97-4844-0\_1.
- [16] Liu, J., Scattarreggia, N., & Malomo, D. (2024). Exploring the seismic performance of corroded RC frames with masonry infills. *Bulletin of Earthquake Engineering*. doi:10.1007/s10518-024-02037-1.
- [17] Rai, A., & Joshi, Y. P. (2014). Applications and properties of fibre reinforced concrete. *Journal of Engineering Research and Applications*, 4(5), 123-131.
- [18] Schwarz, S., Hanaor, A., & Yankelevsky, D. Z. (2015). Experimental response of reinforced concrete frames with AAC masonry infill walls to in-plane cyclic loading. *Structures*, 3, 306-319. doi:10.1016/j.istruc.2015.06.005.
- [19] Messaoudi, A., Chebili, R., Mohamed, H., Furtado, A., & Rodrigues, H. (2024). The In-Plane Seismic Response of Infilled Reinforced Concrete Frames Using a Strut Modelling Approach: Validation and Applications. *Buildings*, 14(7), 1902. doi:10.3390/buildings14071902.
- [20] Harris, H. G., & Sabnis, G. (1999). *Structural modeling and experimental techniques*. CRC Press, Boca Raton, United States. doi:10.1201/9780367802295.
- [21] Šipoš, T. K., & Strukar, K. (2019). Prediction of the seismic response of multi-storey multi-bay masonry infilled frames using artificial neural networks and a bilinear approximation. *Buildings*, 9(5), 121. doi:10.3390/buildings9050121.
- [22] Kyriakides, M. A., & Billington, S. L. (2014). Cyclic response of nonductile reinforced concrete frames with unreinforced masonry infills retrofitted with engineered cementitious composites. *Journal of Structural Engineering*, 140(2), 04013046. doi:10.1061/(ASCE)ST.1943-541X.0000833.
- [23] Folhento, P., Braz-César, M., & Barros, R. (2021). Cyclic response of a reinforced concrete frame: Comparison of experimental results with different hysteretic models. *AIMS Materials Science*, 8(6), 917–931. doi:10.3934/MATERSCI.2021056.
- [24] Shah, S. A. A., Shahzada, K., Gencturk, B., Ullah, Q. S., Hussain, Z., & Javed, M. (2022). In-plane Quasi-static Cyclic Load Tests on Reinforced Concrete Frame Panels with and without Brick Masonry Infill Walls. *Journal of Earthquake Engineering*, 26(11), 5592–5616. doi:10.1080/13632469.2021.1884147.
- [25] Wen, Y. K. (1976). Method for random vibration of hysteretic systems. *Journal of the engineering mechanics division*, 102(2), 249-263. doi:10.1061/JMCEA3.0002106.
- [26] Papia, M., Cavaleri, L., & Fossetti, M. (2003). Infilled frames: Developments in the evaluation of the stiffening effect of infills. *Structural Engineering and Mechanics*, 16(6), 675–693. doi:10.12989/sem.2003.16.6.675.
- [27] Van, T. C., & Lau, T. L. (2020). Experimental Evaluation of Reinforced Concrete Frames with Unreinforced Masonry Infills under Monotonic and Cyclic Loadings. *International Journal of Civil Engineering*, 19(4), 401–419. doi:10.1007/s40999-020-00576-7.
- [28] Teguh, M. (2017). Experimental Evaluation of Masonry Infill Walls of RC Frame Buildings Subjected to Cyclic Loads. *Procedia Engineering*, 171, 191–200. doi:10.1016/j.proeng.2017.01.326.
- [29] Cavaleri, L., Miraglia, N., & Papia, M. (2003). Pumice concrete for structural wall panels. *Engineering structures*, 25(1), 115-125. doi:10.1016/S0141-0296(02)00123-2.
- [30] Caprili, S., Mangini, F., & Salvatore, W. (2015). Evaluation of structural safety and seismic vulnerability of historical masonry buildings: studies and applications in the Tuscany Region. *Structural Studies, Repairs and Maintenance of Heritage Architecture XIV*, 1, 369–380. doi:10.2495/str150311.
- [31] Su, Q., Cai, G., Hani, M., Si Larbi, A., & Tsavdaridis, K. D. (2023). Damage control of the masonry infills in RC frames under cyclic loads: a full-scale test study and numerical analyses. *Bulletin of Earthquake Engineering*, 21(2), 1017–1045. doi:10.1007/s10518-022-01565-y.